JPEDAV (2005) 26:591-604
DOI: 10.1361/154770305X74395
1547-7037/$19.00 ©ASM International

Phase Equilibria and Thermodynamic Properties of the ZrO_2-$GdO_{1.5}$-$YO_{1.5}$ System

O. Fabrichnaya, Ch. Wang, M. Zinkevich, C.G. Levi, and F. Aldinger

(Submitted March 12, 2005; in revised form August 16, 2005)

The thermodynamic description of the ZrO_2-$GdO_{1.5}$-$YO_{1.5}$ system was derived based on binary assessments. One of the binaries ($GdO_{1.5}$-$YO_{1.5}$) was assessed as part of this investigation, another (ZrO_2-$YO_{1.5}$) was reassessed, and the third one (ZrO_2-$GdO_{1.5}$) was adopted directly from a recent report in the literature. The assessments performed incorporated available experimental data on phase equilibria, calorimetric, and vapor pressure measurements. Ternary isothermal sections at 1200, 1400, and 1600 °C were calculated and agreed well with phase equilibria experiments performed as part of this work. The liquidus projection, selected isopleths and a projection of the T_0 surface for the diffusionless tetragonal↔fluorite transformation in the ZrO_2-$GdO_{1.5}$-$YO_{1.5}$ ternary are also reported.

1. Introduction

Yttria-stabilized zirconia (YSZ) has multiple and diverse industrial applications, notably as thermal barrier coatings (TBCs) and electrolytes for solid-oxide fuel cells (SOFCs). Codoping of YSZ by rare earths such as Gd is of interest in thermal barrier systems due to concomitant benefits to the thermal insulating efficiency.[1,2] Compositions about the $Gd_2Zr_2O_7$ pyrochlore compound are also attractive for TBCs because they combine lower thermal conductivity with enhanced microstructural stability upon high-temperature exposure.[3,4] A concern with the latter approach is that compositions with more than ~32%$GdO_{1.5}$ are not thermochemically compatible with the underlying alumina layer in the coating system[5,6] and tend to form interphases at high temperature, with significantly active kinetics at ~1100 °C and above.[5] An approach to circumvent the problem is to add an interlayer of YSZ (~8%$YO_{1.5}$) between $Gd_2Zr_2O_7$ and the underlying alumina.[7] Conversely, the codoped compositions can be designed to be thermochemically compatible, but those that exhibit higher cyclic lives tend to be supersaturated tetragonal solid solutions (t′) that are metastable at the temperatures of practical interest.[7] It has been shown that the phase stability of Y + Gd codoped ZrO_2 compositions depends strongly on the relative Gd:Y ratio and the total amount of stabilizer.[8] It has also been suggested that the trends are related to the magnitude of the driving force for the precipitation process, but no experimental information or thermodynamic models are available to ascertain this hypothesis.

Understanding of the ZrO_2-$YO_{1.5}$-$GdO_{1.5}$ system is thus essential to understand the behavior of novel TBC systems based on $Gd_2Zr_2O_7$/7YSZ bilayers or Y+Gd codoped compositions. The primary aim of this work is to help in developing this understanding by developing a thermodynamic database for the ternary system of interest. The database will be based on the assessed binaries and used to calculate isothermal sections and the liquidus surface for the ternary system. The predicted equilibria will be tested against experimental results.

O. Fabrichnaya, Ch. Wang, M. Zinkevich, and **F. Aldinger,** Max-Planck-Institut für Metallforschung, Heisenbergstr. 3, D-70569, Stuttgart, Germany; and **C.G. Levi,** Materials Department University of California, Santa Barbara, CA 93106-5050. Contact e-mail: fabri@mf.mpg.de.

2. Thermodynamic Modeling

The ThermoCalc software package,[9] based on the Calphad method,[10] is used for the assessment of the thermodynamic parameters and phase diagram calculations in this work. The stable phases in the system ZrO_2-$GdO_{1.5}$-$YO_{1.5}$ and the thermodynamic models used to describe them are shown in Table 1. Because no ternary compounds are found in this system, it should be possible to extrapolate readily from the binary systems into the ternary.

2.1 Binary Systems

The phase diagrams of the ZrO_2-$YO_{1.5}$ and ZrO_2-$GdO_{1.5}$ systems exhibit several important similarities (e.g., wide stability range of fluorite solid solutions, limited range of tetragonal solid solution up to ~6 mol%$MO_{1.5}$, very low solubility of $MO_{1.5}$ in the monoclinic phase). However, the corresponding intermediate compounds $Y_4Zr_3O_{12}$ (δ-phase) and $Gd_2Zr_2O_7$ (pyrochlore) have different (albeit related) structures. In contrast, the system $GdO_{1.5}$-$YO_{1.5}$ exhibits no intermediate binary compound and complete solubility in the bixbyite (C) and hexagonal phases.[11] The other terminal phases have limited solubility of components, with narrow two-phase fields.

Assessments of thermodynamic parameters for the binary systems ZrO_2-$YO_{1.5}$ and ZrO_2-$GdO_{1.5}$ systems are available in the literature.[6,12,13] The work of Chen et al.[12] was not used because the description of stoichiometric ZrO_2 polymorphs was different from that established in a recent reassessment of the Zr-O system[14] and because the high-temperature cubic phase Y_2O_3 was considered in equilibrium with the liquid instead of the hexagonal phase. A

Table 1 Thermodynamic parameters

Phase/temperature range	Model/parameter
FLUORITE (F)	$(Gd^{+3}, Y^{+3}, Zr^{+4})_2(O^{-2}, Va)_4$
298.15-6000	${}^0G^F(Zr^{+4}{:}O^{-2}) - 2{\cdot}HSERZr - 4{\cdot}HSERO = 2{\cdot}GZRO2C$
298.15-6000	${}^0G^F(Zr^{+4}{:}Va) - 2{\cdot}HSERZr = 2{\cdot}GZRO2C - 4{\cdot}GHSEROO$
298.15-6000	${}^0G^F(Gd^{+3}{:}O^{-2}) - 2{\cdot}HSERGd - 4{\cdot}HSERO = GGD2O3L + GHSEROO + 28.818016{\cdot}T - 16{,}929.7864$
298.15-6000	${}^0G^F(Gd^{+3}{:}Va) - 2{\cdot}HSERGd = GGD2O3L - 3{\cdot}GHSEROO + 28.818016{\cdot}T - 16{,}929.7864$
298.15-6000	${}^0G^F(Y^{+3}{:}O^{-2}) - 2{\cdot}HSERY - 4{\cdot}HSERO = GY2O3R + 4000 + GHSEROO + 18.702165{\cdot}T$
298.15-6000	${}^0G^F(Y^{+3}{:}Va) - 2{\cdot}HSERY = GY2O3R - 3{\cdot}GHSEROO + 18.702165{\cdot}T + 4000$
298.15-6000	${}^0L^F(Y^{+3}, Zr^{+4}{:}O^{-2}) = -130{,}802.77 + 50.199044{\cdot}T$
298.15-6000	${}^0L^F(Y^{+3}, Zr^{+4}{:}Va) = -130{,}802.77 + 50.199044{\cdot}T$
298.15-6000	${}^1L^F(Y^{+3}, Zr^{+4}{:}O^{-2}) = 134{,}082.39 - 42.054379{\cdot}T$
298.15-6000	${}^1L^F(Y^{+3}, Zr^{+4}{:}Va) = 134{,}082.39 - 42.054379{\cdot}T$
298.15-6000	${}^0L^F(Gd^{+3}, Zr^{+4}{:}O^{-2}) = -133{,}013 - 14.5394{\cdot}T$
298.15-6000	${}^0L^F(Gd^{+3}, Zr^{+4}{:}Va) = -133{,}013 - 14.5394{\cdot}T$
298.15-6000	${}^1L^F(Gd^{+3},Zr^{+4}{:}O^{-2}) = 91{,}084 - 35.8991{\cdot}T$
298.15-6000	${}^1L^F(Gd^{+3}, Zr^{+4}{:}Va) = 91{,}084 - 35.8991{\cdot}T$
TETRAGONAL (t)	$(Gd^{+3}, Y^{+3}, Zr^{+4})_2(O^{-2}, Va)_4$
298.15-6000	${}^0G^T(Zr^{+4}{:}O^{-2}) - 2{\cdot}HSERZr - 4{\cdot}HSERO = 2{\cdot}GZRO2T$
298.15-6000	${}^0G^T(Zr^{4+}{:}Va) - 2{\cdot}HSERZr = 2{\cdot}GZRO2T - 4{\cdot}GHSEROO$
298.15-6000	${}^0G^T(Gd^{+3}{:}O^{-2}) - 2{\cdot}HSERGd - 4{\cdot}HSERO = GGD2O3L + GHSEROO + 28.818016{\cdot}T - 6929.7964$
298.15-6000	${}^0G^T(Gd^{+3}{:}Va) - 2{\cdot}HSERGd = GGD2O3L - 3{\cdot}GHSEROO + 28.818016{\cdot}T - 6929.7864$
298.15-6000	${}^0G^T(Y^{+3}{:}O^{-2}) - 2{\cdot}HSERY - 4{\cdot}HSERO = GY2O3R + GHSEROO + 18.702165{\cdot}T + 20{,}000$
298.15-6000	${}^0G^T(Y^{+3}{:}Va) - 2{\cdot}HSERY = GY2O3R - 3{\cdot}GHSEROO + 18.702165{\cdot}T + 20{,}000$
298.15-6000	${}^0L^T(Y^{+3}, Zr^{+4}{:}O^{-2}) = -126{,}467.42 + 60{\cdot}T$
298.15-6000	${}^0L^T(Y^{+3}, Zr^{+4}{:}Va) = -126{,}467.42 + 60{\cdot}T$
298.15-6000	${}^0L^T(Gd^{+3}, Zr^{+4}{:}O^{-2}) = -4749 - 42.0515{\cdot}T$
298.15-6000	${}^0L^T(Gd^{+3}, Zr^{+4}{:}Va) = -4749 - 42.0515{\cdot}T$
MONOCLINIC (M)	$(Y^{+3}, Zr^{+4})_2(O^{-2}, Va)_4$
298.15-6000	${}^0G^M(Zr^{+4}{:}O^{-2}) - 2{\cdot}HSERZr - 4{\cdot}HSERO = 2{\cdot}GZRO2M$
298.15-6000	${}^0G^M(Y^{+3}{:}O^{-2}) - 2{\cdot}HSERY - 4{\cdot}HSERO = GY2O3R + 53800 + GHSEROO + 69.5022{\cdot}T$
298.15-6000	${}^0G^M(Y^{+3}{:}Va) - 2{\cdot}HSERY = GY2O3R + 53{,}800 - 3{\cdot}GHSEROO + 69.5022{\cdot}T$
298.15-6000	${}^0G^M(Zr^{+4}{:}Va) - 2{\cdot}HSERZr = 2{\cdot}GZRO2M - 4{\cdot}GHSEROO$
CUBIC_RE2O3 (C)	$(Gd^{+3}, Y^{+3}, Zr^{+4})_2(O^{-2})_3(O^{-2}, Va)_1$
298.15-6000	${}^0G^C(Zr^{4+}{:}O^{-2}{:}O^{-2}) - 2{\cdot}HSERZr - 4{\cdot}HSERO = 2{\cdot}GZRO2C$
298.15-6000	${}^0G^C(Zr^{+4}{:}O^{-2}{:}Va) - 2{\cdot}HSERZr - 3{\cdot}HSERO = 2{\cdot}GZRO2C - GHSEROO$
298.15-6000	${}^0G^C(Gd^{+3}{:}O^{-2}{:}O^{-2})\ 2{\cdot}HSERGd - 4{\cdot}HSERO = GGD2O3C + GHSEROO$
298.15-6000	${}^0G^C(Gd^{+3}{:}O^{-2}{:}Va) - 2{\cdot}HSERGd - 3{\cdot}HSERO = GGD2O3C$
298.15-6000	${}^0G^C(Y^{+3}{:}O^{-2}{:}O^{-2}) - 2{\cdot}HSERGd - 4{\cdot}HSERO = GY2O3R + GHSEROO$
298.15-6000	${}^0G^C(Y^{+3}{:}O^{-2}{:}Va) - 2{\cdot}HSERGd - 3{\cdot}HSERO = GY2O3R$
298.15-6000	${}^0L^C(Gd^{+3}, Zr^{+4}{:}O^{-2}{:}O^{-2}) = 7185 - 6.1943{\cdot}T$
298.15-6000	${}^0L^C(Gd^{+3}, Zr^{+4}{:}O^{-2}{:}Va) = 7185 - 6.1943{\cdot}T$
298.15-6000	${}^0L^C(Y^{+3}, Zr^{+4}{:}O^{-2}{:}O^{-2}) = -34{,}451 + 39.5035{\cdot}T$
298.15-6000	${}^0L^C(Y^{+3}, Zr^{+4}{:}O^{-2}{:}Va) = -34{,}451 + 39.5035{\cdot}T$
B_RE2O3 (B)	$(Gd^{+3}, Y^{+3}, Zr^{+4})_2(O^{-2})_3(O^{-2}, Va)_1$
298.15-6000	${}^0G^B(Zr^{+4}{:}O^{-2}{:}O^{-2}) - 2{\cdot}HSERZr - 4{\cdot}HSERO = 2{\cdot}GZRO2C + 50{,}000$
298.15-6000	${}^0G^B(Zr^{+4}{:}O^{-2}{:}Va) - 2{\cdot}HSERZr - 3{\cdot}HSERO = 2{\cdot}GZRO2C - GHSEROO + 50{,}000$
298.15-6000	${}^0G^B(Gd^{+3}{:}O^{-2}{:}O^{-2}) - 2{\cdot}HSERGd - 4{\cdot}HSERO = GGD2O3B + GHSROO$
298.15-6000	${}^0G^B(Gd^{+3}{:}O^{-2}{:}Va) - 2{\cdot}HSERGd - 3{\cdot}HSERO = GGD2O3B$
298.15-6000	${}^0G^B(Y^{+3}{:}O^{-2}{:}O^{-2}) - 2{\cdot}HSERY - 4{\cdot}HSERO = GY2O3R + GHSEROO + 7725.41022 - 2.77539794{\cdot}T$
298.15-6000	${}^0G^B(Y^{+3}{:}O^{-2}{:}Va) - 2{\cdot}HSERY - 3{\cdot}HSERO = GY2O3R + 7725.41022 - 2.77539794{\cdot}T$
298.15-6000	${}^0L^B(Gd^{+3}, Zr^{+4}{:}O^{-2}{:}O^{-2}) = 74{,}357 - 40.7987{\cdot}T$
298.15-6000	${}^0L^B(Gd^{+3}, Zr^{+4}{:}O^{-2}{:}Va) = 74{,}357 - 40.7987{\cdot}T$
298.15-6000	${}^0L^B(Gd^{+3}, Y^{+3}{:}O^{-2}{:}O^{-2}) = 2024.6874$

(continued)

Table 1 Thermodynamic parameters (continued)

Phase/temperature range	Model/parameter
298.15-6000	${}^0L^{B}(Gd^{+3}, Y^{+3}:O^{-2}:Va) = 2024.6874$
298.15-6000	${}^0L^{B}(Y^{+3}, Zr^{+4}:O^{-2}:O^{-2}) = 100{,}000$
298.15-6000	${}^0L^{B}(Y^{+3}, Zr^{+4}:O^{-2}:Va) = 100{,}000$
A_RE2O3 (A)	$(Gd^{+3}, Y^{+3})_2(O^{-2})_3$
298.15-6000	${}^0G^{A}(Gd^{+3}:O^{-2}) - 2{\cdot}HSERGd - 3{\cdot}HSERO = GGD2O3A$
298.15-6001	${}^0G^{A}(Y^{+3}:O^{-2}) - 2{\cdot}HSERY - 3{\cdot}HSERO = GY2O3R + 2694.9$
HEXAGONAL_RE2O3 (H)	$(Gd^{+3}, Y^{+3}, Zr^{+4})_2(O^{-2})_3(O^{-2}, Va)_1$
298.15-6000	${}^0G^{H}(Zr^{+4}:O^{-2}:O^{-2}) - 2{\cdot}HSERZr - 4{\cdot}HSERO = 2{\cdot}GZRO2C + 50{,}000$
298.15-6000	${}^0G^{H}(Zr^{+4}:O^{-2}:Va) - 2{\cdot}HSRZr - 3{\cdot}HSERO = 2{\cdot}GZRO2C - GHSEROO + 50{,}000$
298.15-6000	${}^0G^{H}(Gd^{+3}:O^{-2}:O^{-2}) - 2{\cdot}HSERGd - 4{\cdot}HSERO = GGD2O3H + GHSEROO$
298.15-6000	${}^0G^{H}(Gd^{+3}:O^{-2}:Va) - 2{\cdot}HSERGd - 3{\cdot}HSERO = GGD2O3H$
298.15-6000	${}^0G^{H}(Y^{+3}:O^{-2}:O^{-2}) - 2{\cdot}HSERY - 4{\cdot}HSERO = GY2O3H + GHSEROO$
298.15-6000	${}^0G^{H}(Y^{+3}:O^{-2}:Va) - 2{\cdot}HSERY - 3{\cdot}HSERO = GY2O3H$
298.15-6000	${}^0L^{H}(Gd^{+3}, Zr^{+4}:O^{-2}:O^{-2}) = 397{,}617 - 189.9203{\cdot}T$
298.15-6000	${}^0L^{H}(Gd^{+3}, Zr^{+4}:O^{-2}:Va) = 397{,}617 - 189.9203{\cdot}T$
298.15-6000	${}^0L^{H}(Gd^{+3}, Y^{+3}:O^{-2}:O^{-2}) = 2235$
298.15-6000	${}^0L^{H}(Gd^{+3}:Y^{+3}:O^{-2}:Va) = 2235$
298.15-6000	${}^0L^{H}(Y^{+3}, Zr^{+4}:O^{-2}:O^{-2}) = 180{,}000$
298.15-6000	${}^0L^{H}IY^{+3}, Zr^{+4}:O^{-2}:Va) = 180{,}000$
X-RE2O3 (X)	$(Gd^{+3}, Y^{+3})_2(O^{-2})_3$
298.15-6000	${}^0G^{X}(Gd^{+3}:O^{-2}) - 2{\cdot}HSERGd - 3{\cdot}HSERO = GGD2O3X$
298.15-6000	${}^0G^{X}(Y^{+3}:O^{-2}) - 2{\cdot}HSERY - 3{\cdot}HSERO = GY2O3H + 1805$
PYROCHLORE (Pyr)	$(Gd^{+3}, Zr^{+4})_2(Gd^{+3}, Zr^{+4})_2(O^{-2}, Va)_6(O^{-2})_1(O^{-2}, Va)_1$
298.15-6000	${}^0G^{Pyr}(Zr^{+4}:Zr^{+4}:O^{-2}:O^{-2}:Va) - 4{\cdot}HSERZr - 7{\cdot}HSERO = GPYROZR - GHSEROO$
298.15-6000	${}^0G^{Pyr}(Gd^{+3}:Zr^{+4}:O^{-2}:O^{-2}:Va) - 2{\cdot}HSERZr - 2{\cdot}HSERGd - 7{\cdot}HSERO = GOPYRO$
298.15-6000	${}^0G^{Pyr}(Zr^{+4}:Gd^{+3}:O^{-2}:O^{-2}:Va) - 2{\cdot}HSERZr - 2{\cdot}HSERGd - 7{\cdot}HSERO = GOPYRO + 170{,}978$
298.15-6000	${}^0G^{Pyr}(Gd^{+3}:Gd^{+3}:O^{-2}:O^{-2}:Va) - 4{\cdot}HSERGd - 7{\cdot}HSERO = 2{\cdot}GOPYRO - GPYROZR + GHSEROO + 170{,}978$
298.15-6000	${}^0G^{Pyr}(Zr^{+4}:Zr^{+4}:Va:O^{-2}:Va) - 4{\cdot}HSERZr - HSERO = 6{\cdot}GPYROGD - 12{\cdot}GOPYRO + 7{\cdot}GPYROZR - 7{\cdot}GHSEROO - 1{,}025{,}867 + 134.8548{\cdot}T$
298.15-6000	${}^0G^{Pyr}(Gd^{+3}:Zr^{+4}:Va:O^{-2}:Va) - 2{\cdot}HSERZr - 2{\cdot}HSERGd - HSERO = 6{\cdot}GPYROGD - 11{\cdot}GOPYRO + 6{\cdot}GPYROZR - 6{\cdot}GHSEROO - 1{,}025{,}867 + 134.8548{\cdot}T$
298.15-6000	${}^0G^{Pyr}(Zr^{+4}:Gd^{+3}:Va:O^{-2}:Va) - 2{\cdot}HSERZr - 2{\cdot}HSERGd - HSERO = 6{\cdot}GPYROGD - 11{\cdot}GOPYRO + 6{\cdot}GPYROZR - 6{\cdot}GHSEROO - 854{,}889 + 134.8548{\cdot}T$
298.15-6000	${}^0G^{Pyr}(Gd^{+3}:Gd^{+3}:Va:O^{-2}:Va) - 4{\cdot}HSERGd - HSERO = 6{\cdot}GPYROGD - 10{\cdot}GOPYRO + 5{\cdot}GPYROZR - 5{\cdot}GHSEROO - 854{,}889 + 134.8548{\cdot}T$
298.15-6000	${}^0G^{Pyr}(Zr^{+4}:Zr^{+4}:O^{-2}:O^{-2}:O^{-2}) - 4{\cdot}HSERZr - 8{\cdot}HSERO = GPYROZR$
298.15-6000	${}^0G^{Pyr}(Gd^{+3}:Zr^{+4}:O^{-2}:O^{-2}:O^{-2}) - 2{\cdot}HSERZr - 2{\cdot}HSERGd - 8{\cdot}HSERO = GOPYRO + GHSEROO$
298.15-6000	${}^0G^{Pyr}(Zr^{+4}:Gd^{+3}:O^{-2}:O^{-2}:O^{-2}) - 2{\cdot}HSERZr - 2{\cdot}HSERGd - 8{\cdot}HSERO = GOPYRO + GHSEROO + 170{,}977.794$
298.15-6000	${}^0G^{Pyr}(Gd^{+3}:Gd^{+3}:O^{-2}:O^{-2}:O^{-2}) - 4{\cdot}HSERAGd - 8{\cdot}HSERO = 2{\cdot}GOPYRO + 2{\cdot}GHSEROO - GPYROZR + 170{,}977.794$
298.15-6000	${}^0G^{Pyr}(Zr^{+4}:Zr^{+4}:Va:O^{-2}:O^{-2}) - 4{\cdot}HSERZr - 2{\cdot}HSERO = 6{\cdot}GOPYRO - 3{\cdot}GPYROGD2 - 2{\cdot}GPYROZR - 6{\cdot}GHSEROO + 174.454{\cdot}T + 710{,}310.4428$
298.15-6000	${}^0G^{Pyr}(Gd^{+3}:Zr^{+4}:Va:O^{-2}:O^{-2}) - 2{\cdot}HSERZr - 2{\cdot}HSERGd - 2{\cdot}HSERO = GOPYRO - 5{\cdot}GHSEROO + 98{,}688.5403 + 134.8548{\cdot}T$
298.15-6000	${}^0G^{Pyr}(Zr^{+4}:Gd^{+3}:Va:O^{-2}:O^{-2}) - 2{\cdot}HSERZr - 2{\cdot}HSERGd - 2{\cdot}HSERO = GOPYRO - 5{\cdot}GHSEROO + 269{,}666 + 134.8548{\cdot}T$
298.15-6000	${}^0G^{Pyr}(Gd^{+3}:Gd^{+3}:Va:O^{-2}:O^{-2}) - 4{\cdot}HSERGd - 2{\cdot}HSERO = 3{\cdot}GPYROGD2 - 4{\cdot}GOPYRO - 4{\cdot}GHSEROO + 2{\cdot}GPYROZR - 341{,}956 + 95.2556{\cdot}T$
Zr3Y4O12 (Z)	$(Zr^{+4})_3(Y^{+3})_4(O^{-2})_{12}$
298.15-6000	${}^0G^{GAM}(Zr^{+4}:Y^{+3}:O^{-2}) = 7{\cdot}GZYO$
IONIC_LIQ (L)	$(Gd^{+3}, Y^{+3}, Zr^{+4})_P(O^{-2})_Q$
298.15-6000	${}^0G^{L}(Zr^{+4}:O - 2) = 2{\cdot}GZRO2L$
298.15-6000	${}^0G^{L}(Gd^{+3}:O - 2) = GGD2O3L$

(continued)

Table 1 Thermodynamic parameters (continued)

Phase/temperature range	Model/parameter
298.15-6000	${}^0G^L(Y^{+3}{:}O-2) = 2{\cdot}GYYLIQ + 3{\cdot}GHSEROO - 1{,}821{,}322.19 + 243.52552{\cdot}T$
298.15-6000	${}^0L^L(Y^{+3}, Zr^{+4}{:}O^{-2}) = 11{,}488$
298.15-6000	${}^1L^L(Y^{+3}, Zr^{+4}{:}O^{-2}) = 1{,}608$
298.15-6000	${}^0L^L Gd^{+3}, Zr^{+4}{:}O^{-2}) = -57{,}043.1057 - 48.6193813{\cdot}T$
298.15-6000	${}^1L^L(Gd^{+3}, Zr^{+4}{:}O^{-2}) = 8{,}116.08904$
298.15-6000	${}^0L^L(Gd^{+3}, Y^{+3}{:}O^{-2}) = 238$
Functions	
298.15-2985	$GZRO2M = -1{,}126{,}367.62 + 426.0761{\cdot}T - 69.6218{\cdot}T{\cdot}\ln(T) - 0.0037656{\cdot}T^2 + 702{,}910.0/T$
2986-6000	$- 1{,}145{,}443.9237 + 567.31299{\cdot}T - 87.864{\cdot}T{\cdot}\ln(T) - 2.54642{\cdot}10^{33}{\cdot}T^{-9}$
298.15-1478	$GZRO2T = - 1{,}117{,}868.813 + 420.27778{\cdot}T - 69.6218{\cdot}T{\cdot}\ln(T) - 0.0037656{\cdot}T^2 + 702{,}910.0/T + 4.589486\ 10^{-21}\ T^7$
1478-2985	$- 1{,}121{,}646.51 + 479.515703{\cdot}T - 78.10{\cdot}T{\cdot}\ln(T)$
2985-6000	$- 1{,}154{,}030.428 + 568.38136\ T - 87.864\ T\ln(T) + 6.092955\ 10^{33}\ T^{-9}$
298.15-1800	$GZRO2C = - 1{,}107{,}276.18 + 416.6337865{\cdot}T - 69.6218{\cdot}T{\cdot}\ln(T) - 0.0037656{\cdot}T^2 + 702{,}910.0/T + 1.920919{\cdot}10^{-21}{\cdot}T^7$
1800-2985	$- 1{,}113{,}681.0 + 491.486437{\cdot}T - 80.0{\cdot}T{\cdot}\ln(T)$
2985-6000	$- 1{,}139{,}763.268 + 563.059458{\cdot}T - 87.864{\cdot}T{\cdot}\ln(T) + 4.90732{\cdot}10^{33}{\cdot}T^{-9}$
298.15-2985	$GZRO2L = - 1027958.268 + 390.79315{\cdot}T - 69.6218{\cdot}T{\cdot}\ln(T) - 0.0037656{\cdot}T^2 + 702{,}910/T + 1.373457{\cdot}10^{-22}{\cdot}T^7$
2985-6000	$- 1{,}050{,}128.04 + 533.11826{\cdot}T - 87.864{\cdot}T{\cdot}\ln(T)$
298.15-6000	$GGD2O3C = - 1{,}868{,}253 + 660.409{\cdot}T - 119.206{\cdot}T{\cdot}\ln(T) - 6.4725{\cdot}10^{-3}{\cdot}T^2 + 780{,}500/T$
298.15-6000	$GGD2O3B = - 1{,}859{,}050 + 632.841{\cdot}T - 116.230099{\cdot}T{\cdot}\ln(T) - 0.0064731233{\cdot}T^2 + 623{,}563.197/T$
298.15-6000	$GGD203A = GGD2O3B + 6300 - 2.5787966{\cdot}T$
298.15-6000	$GGD2O3H = GGD2O3B + 12{,}380 - 5.0294213{\cdot}T$
298.15-6000	$GGD2O3X = GGD2O3B + 18{,}987.5 - 7.5294213{\cdot}T$
298.15-2698	$GGD2O3L = - 1{,}863{,}570.5 + 777.80737{\cdot}T - 132.987058{\cdot}T{\cdot}\ln(T) - 0.010908201{\cdot}T^2 + 1{,}351{,}313.97/T$
2698-6000	$- 1{,}940{,}972 + 1239.328{\cdot}T - 191.476{\cdot}T{\cdot}\ln(T)$
298.15-6000	$GY2O3R = - 1{,}984{,}291 + 763.71851{\cdot}T - 125.692{\cdot}T{\cdot}\ln(T) - 0.00558{\cdot}T^2 + 2{,}344{,}020.5/T - 117{,}305{,}560/T^2$
298.15-6000	$GY2O3H = - 1{,}959{,}291 + 754.10313{\cdot}T - 125.692{\cdot}T{\cdot}\ln(T) - 0.00558{\cdot}T^2 + 2{,}344{,}020.5/T - 117{,}305{,}560/T^2$
298.15-6000	$GOPYRO = - 4{,}163{,}085.95 + 1416.11213{\cdot}T - 248.308422{\cdot}T{\cdot}\ln(T) + 1{,}545{,}056.71/T - 0.022719948{\cdot}T^2$
298.15-6000	$GPYROZR = 4{\cdot}GZRO2C + 93{,}484.8915$
298.15-6000	$GPYROGD = 2{\cdot}GGD2O3C + 64{,}889.5871$
298.15-6000	$GPYROGD2 = 2{\cdot}GGD2O3C + 24{,}520.8115$
298.15-1000	$GHSEROO - 3480.87 - 25.503038{\cdot}T - 11.136{\cdot}T{\cdot}\ln(T) - 0.005098888{\cdot}T^2 + 6.61846\ 10^{-7}\ T^3 - 38{,}365/T$
1000-3300	$- 6568.763 + 12.65988{\cdot}T - 16.8138{\cdot}T{\cdot}\ln(T) - 5.95798\ 10^{-4}{\cdot}T^2 + 6.781\ 10^{-9}{\cdot}T^3 + 262{,}905/T$
3300-6000	$- 13{,}986.728 + 31.259625{\cdot}T - 18.9536\ T\ln(T) - 4.25243{\cdot}10^{-4}{\cdot}T^2 + 1.0721\ 10^{-8}{\cdot}T^3 + 4{,}383{,}200/T$
298.15-2128	$GHSEARZR = - 7827.595 + 125.64905{\cdot}T - 24.1618{\cdot}T{\cdot}\ln(T) - 0.00437791{\cdot}T^2 + 34{,}971/T$
2128-6000	$- 26{,}085.921 + 262.724183{\cdot}T - 42.144{\cdot}T{\cdot}\ln(T) - 1.342895{\cdot}10^{31}{\cdot}T^{-9}$
298.15-1000	$GHSERGD = - 6834.5855 + 9{,}713{,}101{\cdot}T - 24.7214131{\cdot}T{\cdot}\ln(T) - 0.00285240521{\cdot}T^2 - 3.14674076{\cdot}10^{-7}{\cdot}T^3 - 8{,}665.73348/T$
1000-1508.15	$- 6483.25361 + 95.6919924\ T - 24.6598297{\cdot}T{\cdot}\ln(T) - 0.00185225011{\cdot}T^2 - 6.61211607{\cdot}10^{-7}{\cdot}T^3$
1508.15-3600	$- 123{,}124.992 + 699.125537{\cdot}T - 101.800197{\cdot}T{\cdot}\ln(T) + 0.0150644246{\cdot}T^2 - 6.39165948{\cdot}10^{-7}{\cdot}T^3 + 29{,}356{,}890.3/T$
298.15-1000	$GHSERYY = -8011.09379 + 128.572856{\cdot}T - 25.6656992{\cdot}T{\cdot}\ln(T) - 0.00175716414{\cdot}T^2 - 4.17561786{\cdot}10^{-7}{\cdot}T^3 + 26{,}911.509/T$
1000-1795.15	$- 7179.74574 + 114.497104{\cdot}T - 23.4941827{\cdot}T{\cdot}\ln(T) - 0.0038211802{\cdot}T^2 - 8.2534534{\cdot}10^{-8}{\cdot}T^3$
1795.15-3700	$- 67{,}480.7761 + 382.124727{\cdot}T - 56.9527111{\cdot}T{\cdot}\ln(T) + 0.00231774379{\cdot}T^2 - 7.22513088{\cdot}10^{-8}{\cdot}T^3 + 18{,}077{,}162.6/T$
298.15-1000	$GYYLIQ = + 2098.50738 + 119.41873{\cdot}T - 24.6467508{\cdot}T{\cdot}\ln(T) - 0.00347023463{\cdot}T^2 - 8.12981167{\cdot}10^{-7}{\cdot}T^3 + 23{,}713.7332/T$
1000-1795.15	$+ 7386.44846 + 19.4520171{\cdot}T - 9.0681627{\cdot}T{\cdot}\ln(T) - 0.0189533369{\cdot}T^2 + 1.7595327{\cdot}10^{-6}{\cdot}T^3$
1795.15-3700	$- 12{,}976.5957 + 257.400783{\cdot}T - 43.0952{\cdot}T{\cdot}\ln(T)$
298.15-6000	$GZYO = 0.4286{\cdot}GZRO2C + 0.2857{\cdot}GY2O3R - 14550.3912 - 0.520412688{\cdot}T$

recent assessment of the thermodynamic parameters for the system ZrO_2-$YO_{1.5}$ considered the cubic phases with the fluorite (F) and bixbyite (C) structures as one phase having a miscibility gap.[13] The approach, however, is not fully consistent with that used in a recent model of the ZrO_2-$GdO_{1.5}$ system,[6] where the description for the tetragonal and monoclinic phases was also slightly different. Hence, a revision of the ZrO_2-$YO_{1.5}$ binary was undertaken wherein different models are used to describe the F and C solid solutions, and the models for the other ZrO_2 polymorphs are consistent with those used for ZrO_2-$GdO_{1.5}$. The same phase equilibria, calorimetric, and vapor pressure data used in the previous assessment[12] have been applied in the present study to derive the thermodynamic parameters.

The $GdO_{1.5}$-$YO_{1.5}$ system has not been assessed so far, but an experimental phase diagram is available.[11] The latter was used to derive the thermodynamic description of the $GdO_{1.5}$-$YO_{1.5}$ system in the current study.[11] The derived

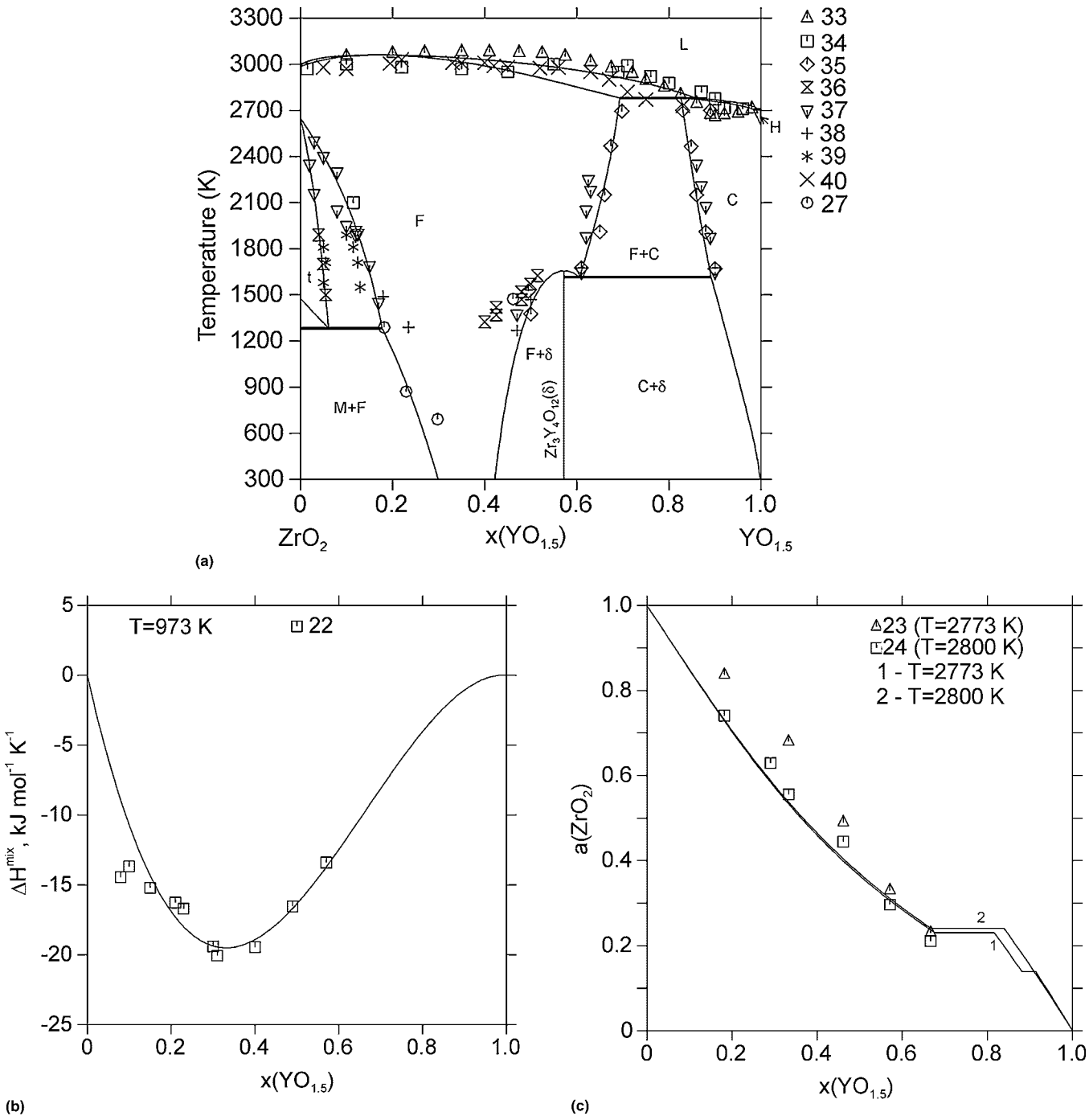

Fig. 1 Phase diagram and property diagram of the ZrO_2-$YO_{1.5}$ system: (a) phase diagram along with data[27,33-40]; (b) enthalpy of mixing in the fluorite phase at 700 °C along with data[22]; (c) activity of ZrO_2 in the fluorite phase along with data[23,24]

thermodynamic parameters are presented in Table 1. It also contains abbreviations of phase names used in the calculated diagrams.

2.2 Thermodynamic Models of Phases

Most of the solid phases are described by the compound energy formalism.[15] The remaining solid phases are treated as stoichiometric compounds. The liquid phase is described by a two-sublattice ionic liquid model.[15]

The fluorite phase (F) is described by two sublattices, one filled by Zr^{+4}, Y^{+3}, and Gd^{+3} cations and the other containing oxygen anions and vacant positions with random occupancy, i.e.:

$$(Zr^{+4},Gd^{+3},Y^{+3})_2\ (O^{-2},Va)_4$$

Table 2 Invariant equilibia in the ZrO_2-Y_2O_3 system

Invariant equilibrium, type	*T*, K	Phase composition, mole fraction of $YO_{3/2}$			Ref
L = F congruent	3060	0.168	0.168	…	This work
	3078	0.374	0.374	…	33
	3024	0.222	0.222	…	40
L + F = C peritectic	2781	0.858	0.693	0.826	This work
	2756	0.901	0.734	0.857	34
	2698	0.890	0.709	0.840	35
L = H + C eutectic	2707	0.994	0.998	0.983	This work
	2653	0.904	0.974	0.824	33
	2606	0.864	…	…	40
	2633	0.907	0.970	0.734	35
$Zr_3Y_4O_{12}$ = F congruent	1657	0.571	0.571	…	This work
	1643	0.571	0.571	…	41
	1648	0.571	0.571	…	36
	1655	0.571	0.571	…	35
F = C + $Zr_3Y_4O_{12}$ eutectoid	1616	0.606	0.893	0.571	This work
	1573	0.630	0.740	0.571	41
	1598	0.620	…	0.571	36
	1650	0.611	0.899	0.571	35
T = F + M eutectoid	1282	0.178	0.001	0.062	This work
	838	…	…	0.075	42
	1273	0.160	0.003	0.020	43
	872	0.23	…	…	27
	1273	0.200	0.003	0.050	31
F = M + $Zr_3Y_4O_{12}$ eutectoid	…	…	…	…	This work
	692	0.298	0.000	0.571	27

In the bixbyite structure (C), the cation sublattice is identical to that of fluorite, but the anion vacancies are ordered, and thus the anionic sublattice is further divided into two sublattices, one completely filled by oxygen anions and another one partly vacant, i.e.,

$$(Gd^{+3},Y^{+3},Zr^{+4})_2\ (O^{-2})_3\ (O^{-2},Va)$$

The structure of the pyrochlore phase is well known.[16-20] It is described for the present purposes by five crystallographically different sublattices with strong preference of cations and anions to each sublattice:

$$(Gd^{+3},Zr^{+4})_2\ (Zr^{+4},Gd^{+3})_2\ (O^{-2},Va)_6\ (O^{-2})\ (Va,O^{-2})$$

The pyrochlore structure is a superstructure of fluorite, but the nature of the order/disorder transition in the ZrO_2-$GdO_{1.5}$ system is still a subject of debate.[5] Some of the literature suggests a continuous ordering transition between fluorite and pyrochlore or hybrid phase containing ordered and disordered regions.[16,17] In this study, the pyrochlore and fluorite are considered as different phases for the purposes of describing their free energy and the transformation as a first-order transition.

The Gibbs energy of a solution phase with mixing in two sublattices (i.e., F, t, C, H) is expressed:

$$G = \sum_i \sum_j Y_i^s Y_j^t G_{i,j} + RT \sum_s \alpha_s \sum_i Y_i^s \ln Y_i^s + \Delta G^{ex}$$

where Y_i^s is the mole fraction of a constituent i in sublattice s, $G_{i,j}$ is Gibbs energy of a compound formed from species i and j, α_s is the number of sites on the sublattice s per mole of formula units of phase, and ΔG^{ex} is the excess Gibbs energy of mixing expressed:

$$\Delta G^{ex} = \sum_s Y_i^s Y_j^s L_{i,j}^s$$

where

$$L_{i,j}^s = \sum_n (Y_i^s - Y_j^s)^n L_{i,j}$$

are the binary interaction parameters in the sublattice s. Interaction parameters with O^{-2} and vacancy in anion sublattice are assumed to be the same for reduction of optimizing parameters.

In the case of more sublattices (i.e., pyrochlore), the Gibbs energy is expressed:

$$G = \sum G_{end} \prod y_j^s + RT \sum \sum \alpha_s y_j^s \ln(y_j^s) + \Delta G^{ex}$$

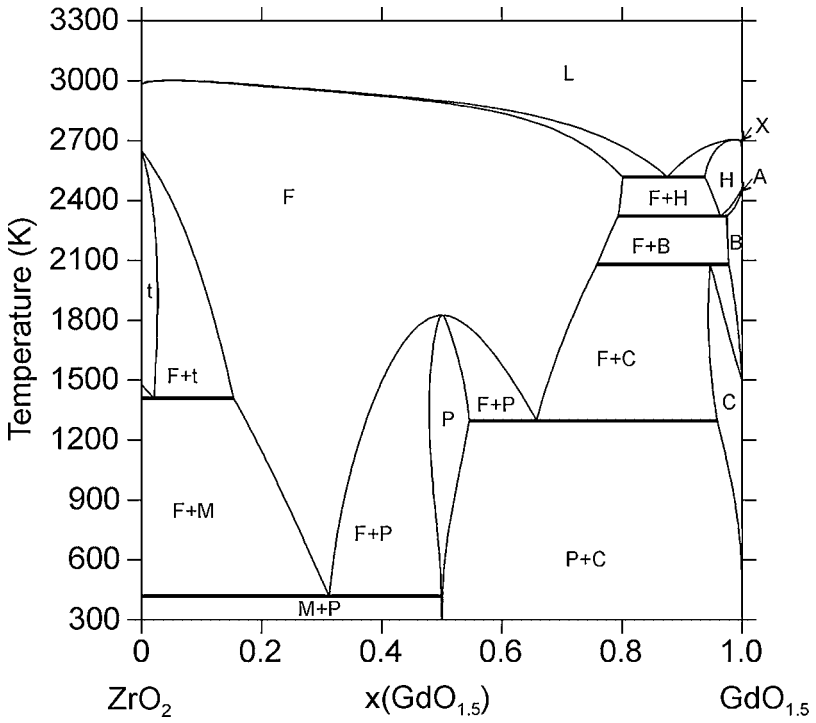

Fig. 2 Phase diagram of the ZrO_2-$GdO_{1.5}$ system

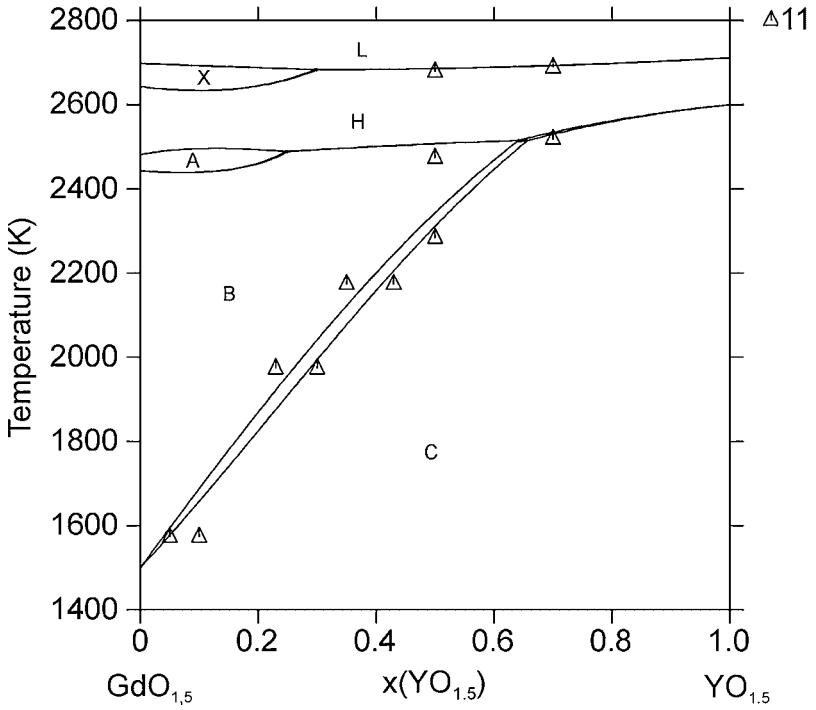

Fig. 3 Phase diagram of the $GdO_{1.5}$-$YO_{1.5}$ system

where G_{end} is the Gibbs energy of the end member compound. The excess energy for pyrochlore is assumed to be zero.

The liquid phase is described by the ionic two-sublattice model[15] $(Gd^{+3},Y^{+3},Zr^{+4})_P(O^{-2})_Q$, where P and Q are the number of sites on the cation and anion sublattices, respectively. The stoichiometric factors P and Q vary with the composition to maintain electroneutrality. The composition dependences of P and Q are expressed:

$$Q = \sum_i v_i y_{C_i} \quad \text{and} \quad P = \sum_j (-v_j y_{A_j}) + Q y_{Va}$$

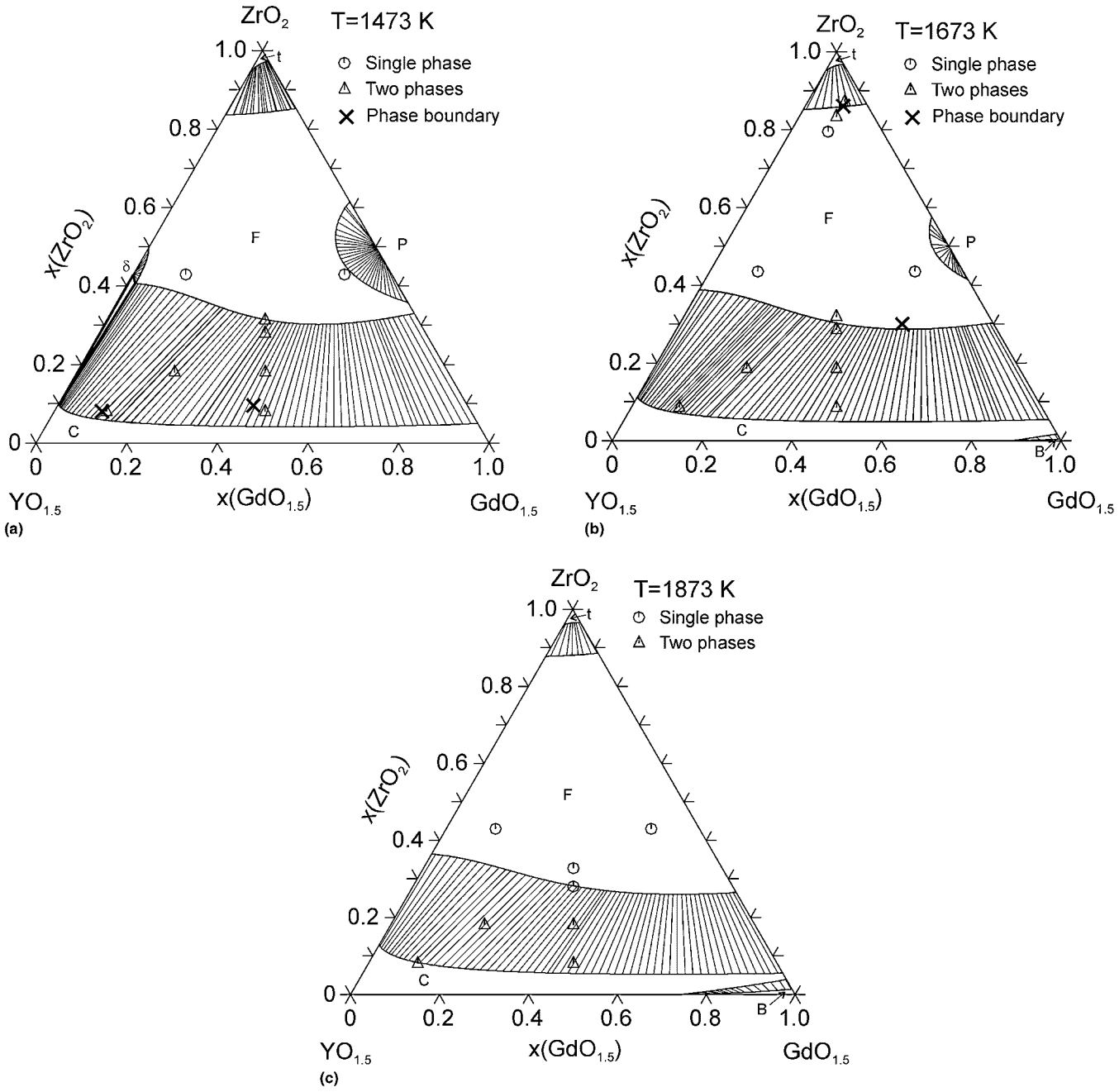

Fig. 4 Isothermal sections of the ZrO_2-$GdO_{1.5}$-$YO_{1.5}$ system: (a) T = 1200 °C, (b) T = 1400 °C, (c) T = 1600 °C

where y_s is the site fraction of species s on a particular sublattice.

3. Experimental Procedures

3.1 Sample Preparation

The samples used in this study were prepared by the reverse coprecipitation method.[21] Assayed solutions of zirconium acetate [$Zr(CH_3COO)_4$, 99.99%], gadolinium nitrate [$Gd(NO_3)_3$, 99.9%], and yttrium nitrate [$Y(NO_3)_3$, 99.9%] were mixed to form the precursor solutions of the desired cation proportions. (All precursors were from Sigma Aldrich. Nitrates supplied as hexahydrate crystals, acetate as liquid.) Each precursor solution was then added in a drop-wise manner (~1 ml/min) to a large volume of ammonium hydroxide solution continuously stirred and maintained at pH = 9 by concurrent addition of ammonia. The precipitation occurred instantaneously as each drop was incorporated into the solution. After the desired volume of precipitate was produced, the suspension was filtered and dried under a heating lamp (~60 °C) to remove most of

the water. The dried precipitates were subsequently pyrolyzed at 1000 °C for 2 h to yield white mixed oxide powders of the desired compositions.

3.2 Sample Treatment and Characterisation

The pyrolyzed powders were isostatically pressed into cylindrical pellets and heat treated in air at high temperature (Pt-crucible, heating and cooling rate 600 °C/h) to achieve equilibration of the phase constitution. Heat treatments were performed at 1200 °C (7 days), 1400 °C (5 days), and 1600 °C (3 days). Heat treatment time was established in previous works[5,6] for similar systems, and it was long enough to reach equilibrium. The phase constitution and compositions were analyzed by x-ray diffraction (XRD) and scanning electron microscopy (SEM).

4. Results

4.1 Calculations

The calculated phase diagram of the ZrO_2-$YO_{1.5}$ system is presented in Fig. 1(a). The corresponding mixing enthalpy and activity data for ZrO_2 in the fluorite phase calculated in this work are presented in Fig. 1(b) and (c) along with experimental data from previous studies.[22-24] The invariant reactions are presented in Table 2 and compared with available experimental data.

The phase diagram of the ZrO_2-$GdO_{1.5}$ system calculated in a previous study[6] is presented in Fig. 2. The corresponding thermodynamic description[6] is accepted in the current study. Diverse kind of experimental information was used in the study[6]: phase equilibria, calorimetric measurements for fluorite, and pyrochlore phases. It should be mentioned that invariant reactions A + H = B and L = H + X are practically degenerated and proceed in $GdO_{1.5}$ composition. The calculated phase diagram of the $GdO_{1.5}$-$YO_{1.5}$ system is presented in Fig. 3 along with experimental data[11] used in the assessment of thermodynamic parameters.

The thermodynamic parameters of the ZrO_2-$GdO_{1.5}$-$YO_{1.5}$ system derived by the combining of binary descriptions are presented in Table 1. The calculated ternary isothermal sections at 1200, 1400, and 1600 °C are presented in Fig. 4(a)-(c), and the projection of the liquidus surface is shown in Fig. 5. There is only one invariant reaction in this system C + L = H + F (U_1) at a temperature of 2316 °C and a liquid composition of 8.6 mol.% ZrO_2 and 61.3 mol.% $GdO_{1.5}$. Univariant reaction L = H + X is practically degenerated and proceeds in the $GdO_{1.5}$-$YO_{1.5}$ system from 70 to 99.9 mol% $GdO_{1.5}$. Isopleths at fixed Gd/(Gd + Y) ratios of 0.25, 0.5, and 0.75 are presented in Fig. 6(a) to (c).

4.2 Experiments

Selected XRD analyses of the samples annealed at 1400 °C are presented in Fig. 7, and a summary of the phases identified in Table 3. Selected samples heat treated at 1400 °C were investigated by SEM/ energy dispersive x-ray (EDX), and the results are compiled in Table 4.

No ternary compounds or three-phase regions were detected, as originally anticipated. In the ZrO_2-rich region, the XRD analysis showed mainly the peaks of fluorite and monoclinic phases. The monoclinic phase is not present at 1400 °C but results from martensitic transformation of the tetragonal phase during cooling. Fluorite is stable as a single phase in a wide composition range. At 1400 °C, at least 5 mol% $GdO_{1.5}$ can be substituted by $YO_{1.5}$ in the pyrochlore structure. However, the XRD analysis could not conclusively ascertain if there is only pyrochlore or a pyrochlore + fluorite phase assemblage in the region nominally denoted as two phase in the thermodynamic model (Fig. 4). The bixbyite phase (C) is continuous along the $GdO_{1.5}$-$YO_{1.5}$ binary for the temperature range of interest. With increasing ZrO_2 content, a two-phase assemblage fluorite + bixbyite becomes stable across the entire range. The maximum concentration of ZrO_2 in the C-phase does not exceed 10 mol%. In the temperature range 1200-1600 °C, the phase boundaries F/F+C and C/F+C appear not to change very much with temperature.

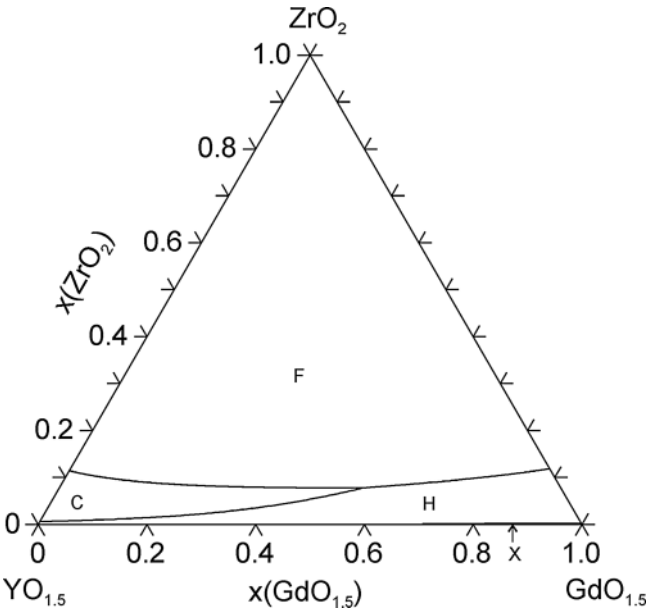

Fig. 5 Liquidus surface of the ZrO_2-$GdO_{1.5}$-$YO_{1.5}$ system

5. Discussion

The experimental results show good agreement with the calculated sections in Fig. 4(a)-(c), indicating that reassessment of the thermodynamic parameters for the ternary is not necessary, and the database derived from the binaries properly represents the behavior of the system in this temperature range.

The similar behavior of the ZrO_2-$YO_{1.5}$ and ZrO_2-$GdO_{1.5}$ systems is reflected in the extension of the common fields across the entire ternary diagram (Fig. 4), with the stability range of the ordered phases limited to the near vicinity of the corresponding binaries. It is well established that Y is too small to form a pyrochlore with ZrO_2, so the destabilization of the pyrochlore with Y substitution for Gd

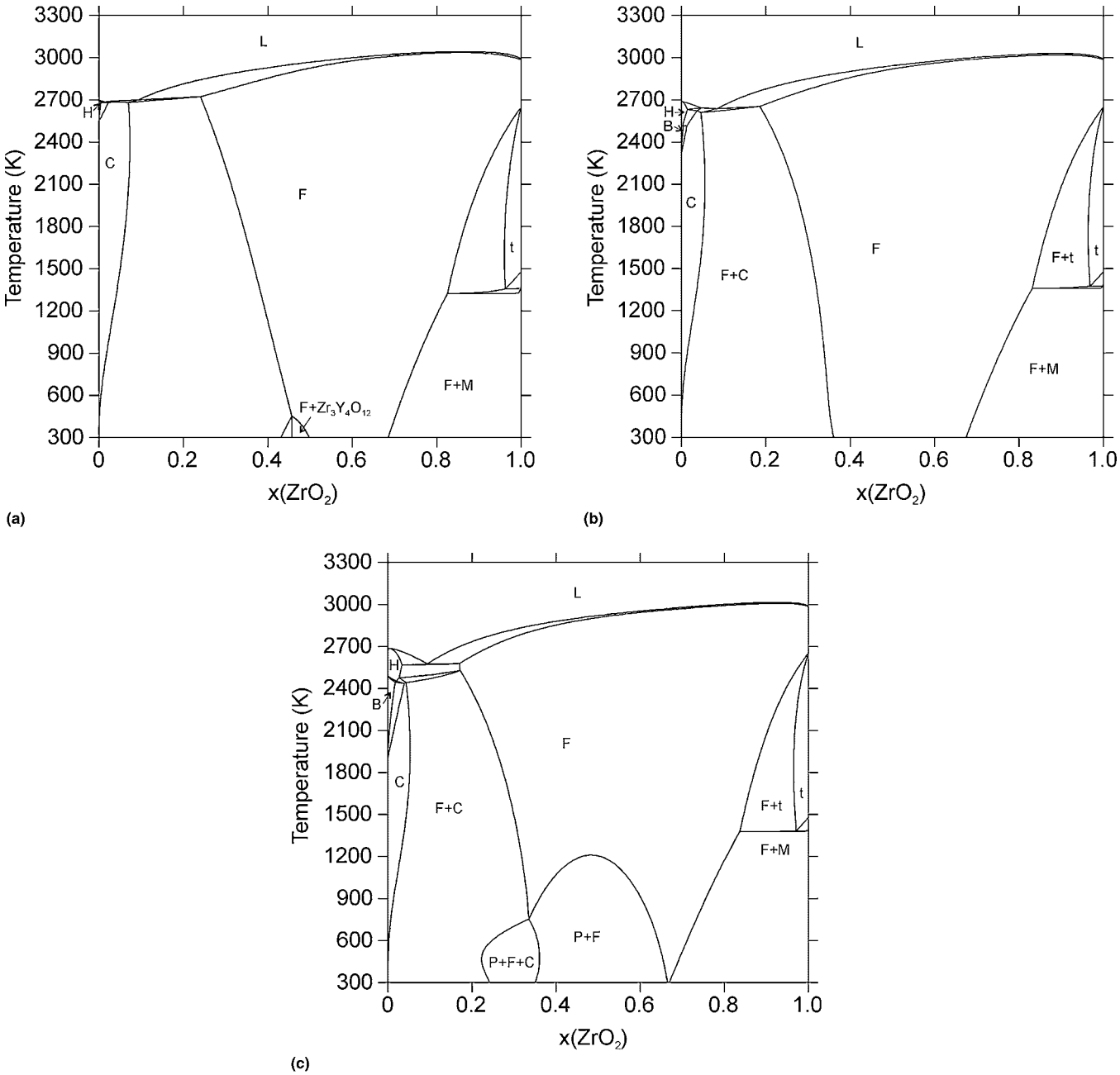

Fig. 6 Isoplethal sections of the ZrO_2-$GdO_{1.5}$-$YO_{1.5}$ system at fixed Gd/(Gd+Y) ratio: (a) 0.25, (b) 0.5, and (c) 0.75

is anticipated. A similar behavior is observed when Zr is substituted for Ti in the $Y_2Ti_2O_7$ pyrochlore. In both cases, the disparity of the A and B cation sizes that favors pyrochlore formation is reduced by the substitution. The ZrO_2-$MO_{1.5}$ (M = Sc, Y, La, rare earth) phase diagrams were calculated in the study of Yokokawa et al.,[25] taking into account correlations based on ionic radii. It was shown that stabilization of pyrochlore zirconates depends on similarity of Zr and M size. Conversely, Y is at the upper end of the range of trivalent cations that form the δ-phase with ZrO_2, the prototype being $Sc_4Zr_3O_{12}$.[7] The moderate stability of this phase is supported by the observation that ordering in $Y_4Zr_3O_{12}$ is relatively weak and sluggish.[26] Hence, substitution of the larger Gd cation for Y is bound to readily destabilize the δ structure. It is somewhat surprising, however, that the single phase fluorite supersedes the potential two phase equilibrium along the $Y_4Zr_3O_{12}$-$Gd_2Zr_2O_7$ down to ambient temperature (Fig. 6a and b). This is probably a consequence of the fact that fluorite is stabilized down to room temperature in the ZrO_2-$YO_{1.5}$ system (Fig. 1). It was shown by Fabrichnaya and Aldinger[13] that the eutectoid reaction $F \leftrightarrow M + \delta$, assumed by Suzuki[27] to occur at 419 °C in ZrO_2-$YO_{1.5}$, is inconsistent with the calorimetric data of Lee et al.[22] Suzuki's data also lead to contradiction

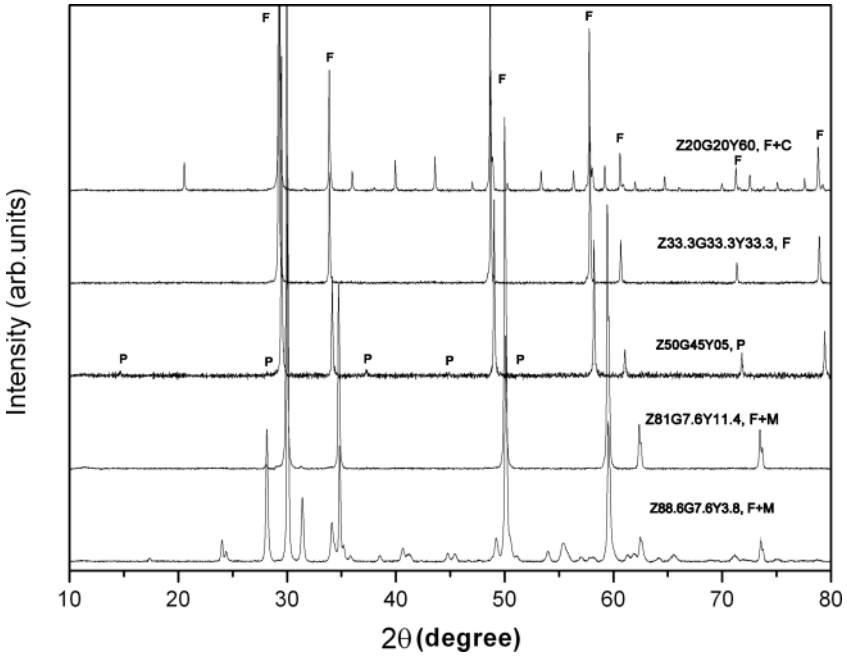

Fig. 7 XRD patterns for the samples heat treated at 1400 °C

Table 3 Summary of the XRD analysis of the samples heat treated at 1200-1600 °C

	Composition, mol.%			Observed phases		
Sample	ZrO_2	$GdO_{1.5}$	$YO_{1.5}$	1200 °C	1400 °C	1600 °C
Z88.6G7.6Y3.8	88.6	7.6	3.8	…	F + M	…
Z88.6G3.8Y7.6	88.6	3.8	7.6	…	F + M	…
Z84.8G7.6Y7.6	84.8	7.6	7.6	…	F + M	…
Z81G7.6Y11.4	81.0	7.6	11.4	…	F	…
Z50G45Y5	50.0	45.0	5.0	…	P	…
Z45G45Y10	45.0	45.0	10.0	F	F	F
Z45G10Y45	45	10	45	F	F	F
Z33G33Y33	33	33	33	F + C	F	F
Z30G35Y35	30	35	35	F + C	F + C	F
Z20G20Y60	20	20	60	C + F	C + F	C + F
Z20G60Y20	20	60	20	…	C + F	…
Z20G40Y40	20	40	40	C + F	C + F	C + F
Z10G10Y80	10	10	80	C + F	C + F	C + F
Z10G45Y45	10	45	45	C + F	C + F	C + F

between the calculated and experimental[28] tie-lines connecting the tetragonal, fluorite, corundum, and YAG phases in the ZrO_2-$YO_{1.5}$-$AlO_{1.5}$ system at 1523 K. The reassessed ZrO_2-$YO_{1.5}$ diagram in Fig. 1 is thus accepted in the current study. It is noted, however, that equilibrium in these systems is unlikely to be reached at temperatures in the range in which the eutectoid reaction $F \leftrightarrow M + \delta$ is reported to occur (~400 °C) and extrapolation of thermodynamic data derived from high-temperature experiments to substantially lower temperatures could also be a source of uncertainty. The eutectic reaction $L \leftrightarrow H + C$ is not reproduced well in calculations made in this study and in work of Chen et al.[12] The reasons could be uncertainties of experimental data at high temperatures and in modeling of the hexagonal phase.

Table 4 SEM/EDX analysis of the samples heat treated at 1400 °C

		Composition, mol.%		
Sample	Phase	ZrO_2	$GdO_{1.5}$	$YO_{1.5}$
Z88.6G7.6Y3.8	F	88.28	7.57	4.15
	M	98.31	1.69	0
Z20G60Y20	F	33.30	50.43	16.27
	C	10.95	60.51	28.54

The isothermal section at 1473K in Fig. 4(a) gives confidence to the approach of using 7YSZ as an intermediate layer to control the interaction between $Gd_2Zr_2O_7$ and the

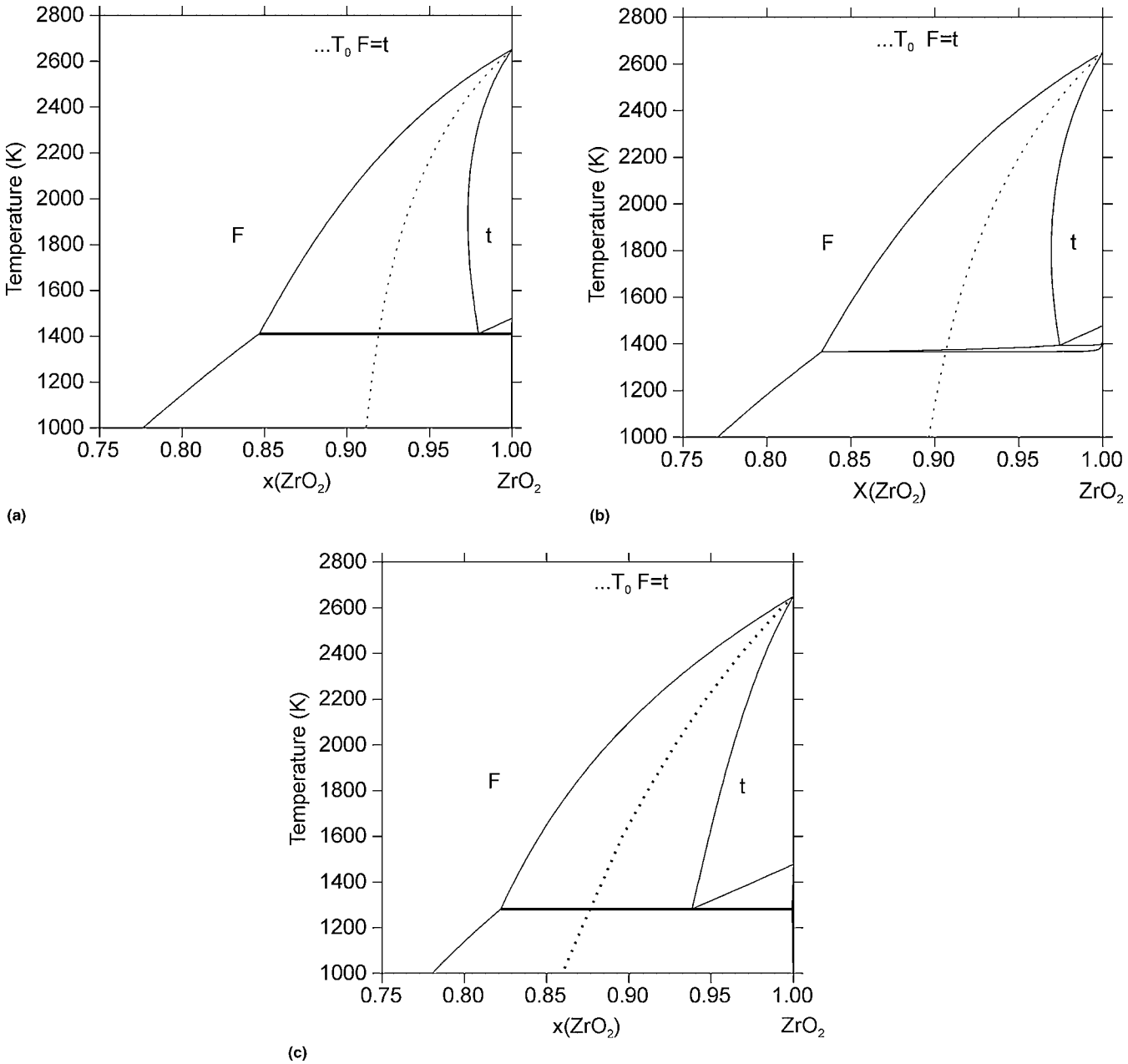

Fig. 8 T_0-lines along with enlarged part of phase diagram at fixed Gd/(Gd + Y) ratio: (a) 0, (b) 0.5, and (c) 1

protective Al_2O_3 in a TBC system, as discussed earlier. Incorporation of Y into $Gd_2Zr_2O_7$ induces disorder, but it is not expected to change significantly the thermal conductivity benefits of the latter.[29] It is less clear, however, how the surface diffusion kinetics that controls sintering would be affected, especially if migration of Y occurs along the internal surfaces of the coating.[30] Conversely, enrichment of Gd in 7YSZ along the tie-line with the pyrochlore would not be expected to move the composition into the regimen in which the phase stability is compromised at the prospective use temperatures (≤1200 °C).

Understanding the broader issue of the stability of supersaturated codoped tetragonal phases used in TBCs requires knowledge of the effects of composition on the F + t phase boundaries and the positions of the T_0 surfaces for the fluorite ↔ tetragonal and tetragonal ↔ monoclinic partitionless transformations.[31] T_0(F/t) corresponds to the intersection point of G-curves of fluorite and tetragonal phases. Traces of the T_0(F/t) surfaces at constant Gd:Y ratios or constant temperatures can be readily calculated with the thermodynamic models generated in this work and are presented in Fig. 8 and 9.

In general, the driving force for the precipitation of fluorite from a supersaturated tetragonal phase depends on the location of its composition relative to the equilibrium tetragonal boundary and the T_0(F/t).[8,32] The calculated te-

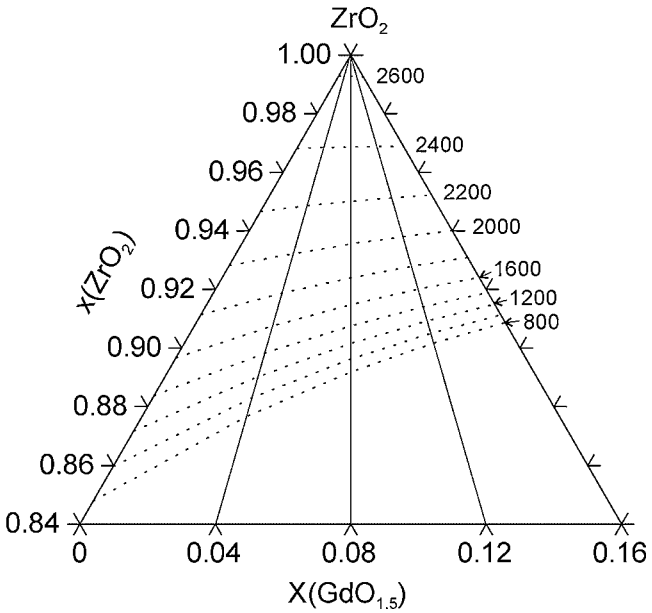

Fig. 9 T_0-lines in the ZrO_2-$GdO_{1.5}$-$YO_{1.5}$ system

tragonal boundary becomes retrograde with the substitution of Gd for Y and shifts to lower concentrations within the temperature range of interest (1200-1500 °C), as depicted in Fig. 8. The T_0(F/t) also shifts to lower concentrations with an increasing level of substitution at a constant temperature, as revealed by Fig. 9. The implication is that with an increasing level of substitution of Gd for Y at the current TBC composition of 7.6%$YO_{1.5}$ the driving force for precipitation will increase across the diagram.

6. Summary

A thermodynamic description of the ZrO_2-$GdO_{1.5}$-$YO_{1.5}$ system was derived based on binary assessments. The ZrO_2-$GdO_{1.5}$ binary was accepted as reported in a recent evaluation, but the ZrO_2-$YO_{1.5}$ system had to be reassessed to enable consistent models for the various solution phases to be used across the ternary. The thermodynamic parameters for the $GdO_{1.5}$-$YO_{1.5}$ binary, previously unavailable, were also derived as part of this work.

The ternary isothermal sections at 1200, 1400, and 1600 °C were calculated and verified by experiments, lending confidence to the thermodynamic models derived. Isopleths at constant Gd:Y ratios and the projection of the ternary liquidus surface were also calculated.

The T_0-lines for the tetragonal/fluorite diffusionless transformation in the ZrO_2-$GdO_{1.5}$-$YO_{1.5}$ system have been calculated, shedding light on previous experimental work on the relative stability of Y + Gd codoped ZrO_2 compositions of interest in thermal barrier coatings. The assessed ternary lends support to the use of YSZ underlayers to prevent thermochemical interactions between $Gd_2Zr_2O_7$ and the thermally grown alumina in a TBC system.

Acknowledgments

This work was financially supported by the HIPERCOAT project of international research collaboration between the European Commission (GRD1-2000-30211) and the U.S. National Science Foundation (DMR-0099685). Ch. Wang is grateful to R.M. Leckie and N.R. Rebollo for assistance in experimental work during his stay at University of California, Santa Barbara. The authors would like to thank F. Predel for technical assistance in performing the SEM analysis.

References

1. J.R. Nicholls, K.J. Lawson, A. Johnstone, and D.S. Rickerby, Methods to Reduce the Thermal Conductivity of EB-PVD TBCs, *Surf. Coat. Technol.,* Vol 151-152, 2002, p 383-391
2. D. Zhu, Y.L. Chen, and R.A. Miller, Defect Clustering and Nano-Phase Structure Characterization of Multi-Component Rare Earth Oxide Doped Zirconia-Yttria Thermal Barrier Coatings, *Ceram. Eng. Sci. Proc.,* Vol 24, 2003, p 525-534
3. M.J. Maloney, Thermal Barrier Coating Systems and Materials, U.S. Patent 6,177,200, (2001)
4. J. Wu, X. Wei, N.P. Padture, P.G. Klemens, M. Gell, E. Garcia, P. Miranzo, and M.I. Osendi, Low-Thermal-Conductivity Rare-Earth Zirconates for Potential Thermal Barrier Coating Applications, *J. Am. Ceram. Soc.,* Vol 85, 2002, p 3031-3035
5. R.M. Leckie, S. Kraemer, M. Ruhle, and C.G. Levi, Thermochemical Compatibility between Alumina and ZrO_2-$GdO_{3/2}$ Thermal Barrier Coatings, *Acta Mater.,* Vol 53, 2005, p 3281-3292
6. S. Lakiza, O. Fabrichnaya, Ch. Wang, M. Zinkevich, and F. Aldinger, Phase Diagram of the ZrO_2-Gd_2O_3-Al_2O_3 System, *J. Eur. Ceramic Soc.,* 2006, in press
7. C.G. Levi, Emerging Materials and Processes for Thermal Barrier Systems. Current Opinion, *Solid State Mater. Sci.,* Vol 8, 2004, p 77-91
8. N. R. Rebollo, O. Fabrichnaya, and C.G. Levi, Phase Stability of Y+Gd Co-doped Zirconia, *Z. Metallkd.,* Vol 94, 2003, p 163-170
9. B. Sundman, B. Jansson, and J.O. Andresson, The Thermo-Calc Databank System, *CALPHAD,* Vol 9, 1985, p 153-196
10. N. Saunders, and P. Miodovnik, *CALPHAD (Calculation of Phase Diagrams): A Comprehensive Guide,* Pergamon, Oxford, UK, 1998
11. A.V. Shevchenko, B.S. Nigmanov, Z.A. Zaitseva, and L.M. Lopato, Interaction of Samarium and Gadolinium Oxides with Yttrium Oxide, *Inorg. Mater.,* Vol 22, 1986, p 681-685
12. M. Chen, B. Hallstedt, and L.J. Gauckler, Thermodynamic Modelling of the ZrO_2-$YO_{1.5}$ System, *Solid State Ionics,* Vol 170, 2004, p 255-274
13. O. Fabrichnaya, and F. Aldinger, Assessment of Thermodynamic Parameters in the System ZrO_2-Y_2O_3-Al_2O_3, *Z. Metallkd.,* Vol 95, 2004, p 27-39
14. Ch. Wang, M. Zinkevich, and F. Aldinger, Comments on the Thermodynamic Modeling of Zr-O System, *CALPHAD,* Vol 28, 2004, 281-292
15. M. Hillert, The Compound Energy Formalism, *J. Alloys Comp.,* Vol 320, 2001, p 161-176
16. T. Van Dijk, K. J. de Vries, and A.J. Burggraaff, Electrical Conductivity of Fluorite and Pyrochlore $Ln_xZr_{1-x}O_{2-x/2}$ (Ln = Gd,Nd) Solid Solutions, *Phys. Stat. Sol. (a),* Vol 58, 1980, p 115-125
17. T. Uehara, K. Koto, and F. Kanamaru, Stability and Antiphase Domain Structure of the Pyrochlore Solid Solutions in the ZrO_2-Gd_2O_3 System, *Solid State Ionics,* Vol 23, 1987, p 137-143
18. C. Ceder, A.F. Kohan, and M.K. Aydinol, P.D. Tepisch, and A. Van der Ven, Thermodynamics of Oxides with Substitu-

tional Disorder: a Microscopic Model and Evaluation of Important Energy Contributions, *J. Am. Ceram. Soc.,* Vol 81, 1998, p 517-525
19. P.J. Wilde and C.R.A. Catlow, Defects and Diffusion in Pyrochlore Structured Oxides, *Solid State Ionics,* Vol 112, 1998, p 173-183
20. M. Pirzada, R.W. Grimes, L. Minervini, J.F. Maguire, and K.E. Sickafus, Oxygen Migration in $A_2B_2O_7$ Pyrochlores, *Solid State Ionics,* Vol 140, 2001, p 201-208
21. M. Ciftcioglu and M.J. Mayo, Processing of Nanocrystalline Ceramics, *Superplasticity in Metals, Ceramics and Intermetallics, Mater. Res. Soc. Symp. Proc. 196,* M.J. Mayo, M. Kobayashi, and J. Wadsworth, Ed., MRS, Pittsburgh, PA, 1990), p 77
22. T.A. Lee, A. Navrotsky, and I. Molodetsky, Enthalpy of Formation of Cubic Yttria-Stabilized Zirconia, *J. Mater. Res.,* Vol 18, 2003, p 908-918
23. A.N. Belov and G.A. Semenov, Thermodynamics of Binary Solid Solutions of Zirconium, Hafnium, and Yttrium Oxides from High-Temperature Mass Spectrometry Data, *Russ. J. Phys. Chem.,* Vol 59, 1985, 342-344
24. K.N. Marushkin and A.S. Alikanyan, The Quasibinary Systems HfO_2-ZrO_2, ZrO_2-Y_2O_3 and HfO_2-Y_2O_3, *Russ. J. Inorg. Chem.,* Vol 36, 1991, 1481-1484
25. H. Yokokawa, N. Sakai, T. Kawada, and M. Dokiya, Phase Diagram Calculations for ZrO_2 Based Ceramics: Thermodynamic Regularities in Zirconate Formation and Solubility of Transtion Metal Oxides, *Science and Technology of Zirconia V,* S.P.S. Badwal, M.J. Bannister, and R.H.J Hannink, Ed., The Australian Ceramic Society, The Technomic Publication Co. Inc., Lancaster, PA, 1993, p 59-68
26. H.G. Scott, The Yttria-Zirconia δ Phase, *Acta Crystall.,* Vol 33 B, 1977, p 281-282
27. Y. Suzuki, Phase Transition Temperature of Fluorite-Type ZrO_2-Y_2O_3 Solid Solutions Containing 8-44 mol% Y_2O_3, *Solid State Ionics,* Vol 81, 1995, p 211-216
28. L.M. Lopato, L.V. Nazarenko, G.V. Gerasimjuk, and A.V. Shevchenko, Isothremal Section of the ZrO_2-Y_2O_3-Al_2O_3 Phase Diagram at 1250 °C, *Inorg. Mater.,* Vol 28, 1992, p 644-647
29. J. Wu, N.P. Padture, P.G. Klemens, M. Gell, E. Garcia, P. Miranzo, and M.I. Osendi, Thermal Conductivity of Ceramics in the ZrO_2-$GdO_{1.5}$ System, *J. Mater. Res.,* Vol 17, 2002, p 3193-3200
30. A.S. Gandhi, R.M. Leckie, S. Kraemer, and C.G. Levi, Bi-Layer Concept to Control the Interaction between Gd Zirconate and the Thermally Grown Oxide in a TBC System (private communication) 2005, University of California, Santa Barbara
31. M. Yashima, M. Kakihana, and M. Yoshimura, Metastable-Stable Phase Diagrams in the Zirconia-Containing Systems Utilized in Solid-Oxide Fuel Cell Application, *Solid State Ionics,* Vol 86-88, 1996, p 1131-1149
32. N.R. Rebollo, A.S. Gandhi, and C.G. Levi, Phase Stability Issues in Emerging TBC Systems, *High Temperature Corrosion and Materials Chemistry IV*, E.J. Opila, P. Hou, T. Maruyama, B. Pieraggi, M. McNallan, D. Shifler, and E. Wuchina, Ed., *Electrochem. Soc. Proc.,* Vol PV-2003-16, 2003, p 431-442
33. A. Rouanet, High Temperature Solidification and Phase Diagrams of the ZrO_2-Er_2O_3, ZrO_2-Y_2O_3, and ZrO_2-Yb_2O_3 System, *C.R. Seances Acad. Sci.,* Ser C, Vol 267, 1968, p 1581-1584
34. S.R. Skaggs, "The ZrO_2-Y_2O_3 System above 2000° C," Ph.D. Thesis, New Mexico State University, Albuquerque, N.M., 972
35. V.S. Stubican, R.C. Hink, and S.P. Ray, Phase Equilibria and Ordering in the System ZrO_2-Y_2O_3, *J. Am. Ceram. Soc.,* Vol 61, 1978, p 17-21
36. C. Pascual and P. Duran, Subsolidus Phase Equilibria and Ordering in the System ZrO_2-Y_2O_3, *J. Am. Ceram. Soc.,* Vol 66, 1983, p 23-27
37. V.S. Stubican, Phase Equilibria and Metastabilities in the Systems ZrO_2-MgO, ZrO_2-CaO, and ZrO_2-Y_2O_3, *Advances in Ceramics, Vol. 24 Science and Technology of Zirconia III,* S. Somiya, N. Yamamoto, and H. Hanagida, Ed., Am. Ceram. Soc., Columbus, OH, 1988, p 71-82
38. K. Nakamura, S. Hirano, and S. Somiya, The System ZrO_2-Y_2O_3 under Hydrothermal Condition at 1000 kg/sm^2, *Yogyo Kyokasishi,* Vol 83, 1975, p 570-574 (in Japanese)
39. M. Ruehle, N. Claussen, and A.H. Heuer, Microstructural Studies of Y_2O_3-Containing Tetragonal ZrO_2 Polycrystals (Y-TZP), *Advances in Ceramics Vol. 12 Science and Technology of Zirconia II,* N. Claussen, M. Ruehle, A.H. Heuer, Ed., Am. Ceram. Soc. Columbus, OH, 1984, p 352-370
40. T. Noguchi, M. Muzino, and T. Yamada, The Liquidus Curve of the ZrO_2-Y_2O_3 System as Measured by a Solar Furnace, *Bull. Chem. Soc. Jpn.,* Vol 43, 1970, p 2614-2616
41. H.G. Scott, The Phase Relationships in the Yttria-Rich Part of the Yttria-Zirconia System, *J. Mater. Sci.,* Vol 10, 1975, p 311-316
42. K.K. Srivastava, R.N. Patil, C.B. Choudhary, K.V.G.K. Gokhale, and E.C. Subbarao, Revised Phase Diagram of the System ZrO_2-$YO_{1.5}$, *Trans. Br. Ceram. Soc.,* Vol 73, 1974, p 85-91
43. N. Yashikawa, H. Eda, and H. Suto, On the Cubic/Teteragonal Phase Equilibrium of the ZrO_2-Y_2O_3 System, *J. Jpn. Inst. Met.,* Vol 50, 1986, p 113-118